

Electronic Supplementary Information (ESI)

Direct microencapsulation of pure polyamine by integrating microfluidic emulsion and interfacial polymerization for practical self-healing materials

He Zhang,^{a,b} Xin Zhang,^c Chenlu Bao,^d Xin Li,^e Dawei Sun,^{f,g} Fei Duan,^b Klaus Friedrich,^h Jinglei Yang^{f*}

^a The National Engineering Research Center of Novel Equipment for Polymer Processing, The Key Laboratory of Polymer Processing Engineering (SCUT), Ministry of Education, School of Mechanical and Automotive Engineering, South China University of Technology, Guangzhou, China, 510641

^b School of Mechanical and Aerospace Engineering, Nanyang Technological University, 639798, Singapore

^c School of Civil and Environmental Engineering, Nanyang Technological University, 639798, Singapore

^d School of Materials Science and Engineering, Tianjin Polytechnic University, Tianjin, 300387, China

^e National Laboratory of Solid State Microstructures and Department of Materials Science and Engineering, Nanjing University, Nanjing 210093, China

^f Department of Mechanical and Aerospace Engineering, Hong Kong University of Science and Technology, Kowloon, Hong Kong, China

^g College of Materials Science and Engineering, Beijing University of Technology, Beijing 100124, China

^h Institute for Composite Materials, Technical University of Kaiserslautern, Kaiserslautern, D-67663 Germany

*Corresponding author. Email: maeyang@ust.hk

Experimental session

1. Materials

Tetraethylenepentamine (TEPA), decalin, *n*-hexadecane, cyclohexane, 4,4'-methylenebis(cyclohexyl isocyanate) (HMDI, mixture of isomers), catalyst 1,4-diazabicyclo[2.2.2]octane (DABCO), bisphenol F diglycidyl ether (BFDGE), butyl glycidyl ether (BGE), urea, 37wt% formaldehyde solution, formic acid, and poly(ethylene-*alt*-maleic anhydride) copolymer (M_w 100,000-500,000), were purchased from Sigma-Aldrich. Epolam 5015 and Hardener 5015 were supplied by Axson. JEFFAMINE T403 is a free sample from Huntsman. Arlacel P135 was purchased from Croda. Microbore polytetrafluoroethylene tubing, T1 (I.D.: 0.012 inch; O.D.: 0.03 inch) and T2 (I.D.: 0.022 inch; O.D.: 0.042 inch), were purchased from Cole-Parmer. All reagents were used as received.

2. Fabrication of pure polyamine microcapsule

Microfluidic T-junction was carefully manufactured by inserting T1 into T2 (T1/T2) and sealing the junction tightly. Length from the junction to the end outlet of T2 is ~30mm. Polyamine was syringed through T1 at feeding rate of 0.02ml/min, and co-flow solvent, *n*-hexadecane, with 1wt% Arlacel P135 as surfactant, was syringed through T2 at feeding rate of 0.5ml/min. The mixture after T-junction flowed into the reaction solution agitated gently by a three-blade propeller at 120rpm. The reaction solution contains 50.0ml decalin, 6.0g HMDI, 0.5g Arlacel P135, and 0.5g DABCO. After addition of ~12.0ml *n*-hexadecane, the generation of amine droplets was ceased, and the mixture was allowed to react at 40°C for 1h, 50°C for 2h, and 60°C for 2h in order under agitation of 200rpm to thicken the shell. And finally the polyamine microcapsules were rinsed with pure cyclohexane for 4-5 times, dried for 5-10min, and finally collected.

During one typical process, a high-speed camera (Fastec Imaging with lens Micro-NIKKOR) was used to observe generation of amine droplets and evolution of droplets to preliminary microcapsules in reaction solution.

3. Fabrication of epoxy microcapsule containing F10B

Epoxy microcapsules was fabricated by *in-situ* polymerization of urea-formaldehyde pre-polymer in an oil-in-water emulsion following a protocol established by Jin *et al.*¹ The agitation rate adopted for emulsification is 800rpm. The as-achieved epoxy microcapsules were further subjected to another strengthening process using urea-formaldehyde pre-polymer developed by Sun *et al.*² to improve their strength and tightness. They were strengthened at 55°C for 3h during the process.

4. Quantification of self-healing performance

Healing performance of self-healing epoxy was characterized using tapered double cantilever beam (TDCB) specimen (**Fig. 4a**).³ TDCB frame with a short groove for filling of formulated self-healing epoxy was fabricated by curing Epolam 5015 with Hardener 5015 (100:30) firstly at room temperature (RT ~22-25°C) for 24h and then at 35°C for another 24h. Formulated self-healing epoxy mixture, Epolam 5015 and Hardener 5015 (100:30) containing dual microcapsules with compositions shown in Table S1, was poured into the short groove and cured at RT for 24h followed by 35°C for another 24h.

The mode I fracture toughness test was carried out using an Instron testing machine (Instron Mini High Precision Tester). A pre-crack was made by a sharp blade before the fracture toughness test. Loading speed of 1mm/min was adopted for the test. After fracture, the specimens were healed at RT for 48h. Healing tests were performed using the same machine

and parameters. Herein, since the fracture toughness using TDCB geometry is independent of crack length and proportional to the peak load,³ healing efficiency could be defined as:

$$\eta = 100\% \cdot \frac{K_{IC}^{Healed}}{K_{IC}^{Original}} = 100\% \cdot \frac{P_{Average}^{Healed}}{P_{Average}^{Original}} \quad \backslash * \text{MERGEFORMAT (1)}$$

where $P_{Average}^{Healed}$ and $P_{Average}^{Original}$ are the averaged healed peak load and averaged original peak load.

At least 4 pieces of specimens for each composition were tested to obtain an averaged value with standard deviation.

To test the thermal and long-term stability, self-healing specimens with optimized composition was subjected to different post-curing conditions and aging durations at RT (**Table S1**). To check the healing kinetics, one set of specimens were healed at RT for different durations (**Table S1**).

5. Characterization methods

Morphology, structure, and size distribution of the obtained microcapsules were characterized using field emission scanning electronic microscope (FESEM, JOEL JSM-7600F). Extraction of TEPA microcapsules was identified by Fourier-transform infrared (FTIR, Varian 3100) using transmittance mode. Spectra in range from 400cm^{-1} to 4000cm^{-1} were used. Composition and thermal stability of microcapsules were characterized using thermogravimetric analysis (TGA, AutoTGA Q500). In TGA tests, 10-30mg powder or liquid sample was placed in a platinum pan and heated to 600°C under nitrogen atmosphere with ramp rate of $10^{\circ}\text{C}/\text{min}$. Proton nuclear magnetic resonance (^1H NMR) was used to analyze chemical composition of core materials using a Bruker BBFO (400 MHz) spectrometer. Chemical shifts were recorded in parts per million (ppm, δ) relative to chloroform ($\delta = 7.26$).

Supplementary Text

1. Theoretical fitting of microcapsule size in Fig. 2b

The theoretical fitting of microcapsule size regarding feeding rate in **Fig. 2b** was achieved by volume transformation between the adopted feeding rate (V) and the reference feeding rate (V_0 , 0.005ml/min). Firstly, several assumptions are made as follows:

- 1, Size of microcapsules is equal to that of the corresponding polyamine droplets;
- 2, During generation of polyamine droplets in the T-junction at different feeding rates for polyamine, the generated number of droplet (N) in given time (t) is independent of feeding rate. It means that feeding rate only influences the size of droplets, but not the number of generated droplets;
- 3, Within the investigated range of feeding rates (0.005-0.075ml/min), diameter of tubing T1 is big enough for the flowing of polyamine stream.

At the reference feeding rate (V_0), the diameter (\bar{d}_0) of droplets is:

$$V_0 \cdot t = N_0 \frac{4}{3} \pi \left(\frac{\bar{d}_0}{2} \right)^3 \quad \backslash * \text{MERGEFORMAT (1)}$$

where N_0 is the total number of droplets generated in time t when feeding rate V_0 is used. When a feeding rate of V is adopted, the diameter of droplets (\bar{d}) is:

$$V \cdot t = N \cdot \frac{4}{3} \pi \left(\frac{\bar{d}}{2} \right)^3 \quad \backslash * \text{MERGEFORMAT (2)}$$

where N is the total number of droplets generated in time t when feeding rate V is used. Based on Equation (1) and (2), diameter of droplets at feeding rate V can be expressed as:

$$\bar{d} = \sqrt[3]{\frac{V}{V_0}} \cdot \sqrt[3]{\frac{N_0}{N}} \cdot \bar{d}_0 \quad \backslash* \text{MERGEFORMAT (3)}$$

When the number of generated droplets does not vary with feeding rate, diameter of the droplet/microcapsule at V is:

$$\bar{d} = \sqrt[3]{\frac{V}{V_0}} \cdot \bar{d}_0 \quad \backslash* \text{MERGEFORMAT (4)}$$

Supplementary Figure Captions

Fig. S1 Reaction scheme between polyamine and diisocyanate (HMDI). Due to the extremely high reactivity of amine with isocyanate, instant reaction occurs when the two monomers meet with each other near interface. The encapsulation strategy takes advantage of this feature to form the shell and avoid loss of polyamine in the core by using excessive amount of HMDI in reaction solution.

Fig. S2 Schematic molecular structures of polyamines for encapsulation, i.e. TEPA and JEFFAMINE T403. TEPA is condensate of ethylenediamine, whereas JEFFAMINE T403 is a commercial trifunctional primary amine with repeated soft oxypropylene units in its molecular structure. Due to the relatively soft chain and low functionality of JEFFAMINE T403 in comparison with those of TEPA, epoxy cured by JEFFAMINE T403 has higher fracture toughness, which is crucial for brittle epoxy.

Fig. S3 Influence of T-junction location on morphology and quality of the products. (a) Optical microscopic image showing fibre with liquid polyamine core when the T-junction is too close to the end outlet of T2. In this case, the thin continuous polyamine stream is not able to break down into individual polyamine droplets. Once the polyamine stream contacts with reaction solution, it is enwrapped by polyurea wall owing to the rapid interfacial polymerization between polyamine in the stream and diisocyanate in the reaction solution at interface, leading to formation of fibre with liquid polyamine core. (b) Polyurea generated around polyamine droplets or in reaction solution when the T-junction locates too far away from the end outlet of T2. While the former causes agglomeration of microcapsules in the subsequent encapsulation process easily, the latter turns to polyurea debris in the collected final microcapsules to decrease their quality.

Fig. S4 Easy tailoring of core compositions of microcapsules obtained by the proposed method. Morphology, core-shell structure and double-walled structure of microcapsules containing 50TEPA50T403 (a-c) and 25TEPA75T403 (d-f), respectively. The FESEM images show that amine mixtures of 50TEPA50T403 and 25TEPA75T403 can be successfully encapsulated and the achieved microcapsules are quite similar to that containing pure TEPA. It demonstrates that the designed encapsulation process is not selective to the physicochemical properties of the polyamines for encapsulation.

Fig. S5 Thermal stability of TEPA and JEFFAMINE T403 at 100°C. During the tests, pure TEPA and JEFFAMINE T403 were treated isothermally at 100°C to monitor their weight loss. While TEPA gradually evaporates or decomposes in ~10h, JEFFAMINE T403 is much more stable at 100°C. Only ~13wt% of JEFFAMINE T403 evaporates or decomposes after ~12h at 100°C.

Fig. S6 Schematic molecular structures of BFDGE and BGE in epoxy mixture for encapsulation. In contrast to bisphenol A diglycidyl ether (BADGE), BFDGE has a relatively lower viscosity, which is beneficial to the encapsulation process. However, cured epoxy based on BFDGE has a comparable mechanical strength and higher fracture toughness to that based on BADGE. Consequently, BFDGE was selected as the epoxy monomer for encapsulation.

Fig. S7 Epoxy microcapsule containing F10B. The microcapsules were synthesized by *in-situ* polymerization of urea-formaldehyde pre-polymer in an oil-in-water emulsion with agitation rate of 800rpm, and then strengthened by another process using urea-formaldehyde pre-polymer. Just like other poly(urea-formaldehyde) (PUF) microcapsules with different core materials, this epoxy microcapsule has a rough outer surface and a smooth inner surface.

However, the inner wall is much thicker in contrast to that of PUF microcapsule obtained by protocol established by Brown *et al.* ⁴

Fig. S8 TGA curves of pure BGE, pure BFDGE, and epoxy microcapsule with F10B.

Although BGE evaporates away completely before $\sim 150^{\circ}\text{C}$, the epoxy microcapsule does not show evident weight loss before 200°C , which demonstrates the high tightness of the PUF shell and high thermal stability of the epoxy microcapsule.

Fig. S9 Dispersion and distribution of the dual microcapsules in epoxy host matrix.

The specimen contains 5wt% amine microcapsule and 5wt% epoxy microcapsule. Although randomly, both microcapsules can be dispersed uniformly in the host matrix.

Fig. S10 Influence of polyamine composition in amine microcapsule on healing performance of the self-healing epoxy.

(a) Healing performance regarding ratio variation of dual microcapsules respectively containing pure TEPA and F10B. Only one effective datum was collected from four specimens for ratio of 1:3, and no effective data were collected for ratio of 1:4. (b) Healing performance regarding ratio variation of dual microcapsules respectively containing 50TEPA50T403 and F10B. The highest healing efficiencies for these two self-healing systems are $24.5\pm 2.4\%$ (Ratio of 1:2) and $75.2\pm 6.5\%$ (Ratio of 2:3), respectively. In stark contrast to healing performance with full recoverability for amine microcapsule containing 25TEPA75T403, healing in these two systems are much poorer. With increasing concentration of TEPA (and decreasing concentration of JEFFAMINE T403), the healing performance decreases dramatically due to the poorer fracture toughness of cured epoxy by TEPA in comparison to that by JEFFAMINE T403. This observation demonstrates the importance of tailoring core composition of the adopted microcapsules for self-healing, which

is an evident superiority of the invented encapsulation technique. By integrating microfluidic T-junction and interfacial polymerization, this technique is capable of encapsulating polyamines irrelevant to their physicochemical properties.

Fig. S11 Fractograph showing the mirrored fracture surfaces of crack after healing test of the self-healing epoxy using TDCB specimen at optimized condition (10wt%, 1:1).

Fig. S12 Fractograph of control specimens. (a) Crack surface of TDCB specimen by rinsing away the released healants using acetone before healing. Smooth surface, fractured epoxy microcapsules and amine microcapsules can be observed on surface of specimen. It can be seen that it is totally different from the fractured surface of healed specimen; and (b) Crack surface of TDCB specimen with only 10wt% epoxy microcapsules containing F10B. It is covered by a thin layer of liquid epoxy film with the absence of amine microcapsule.

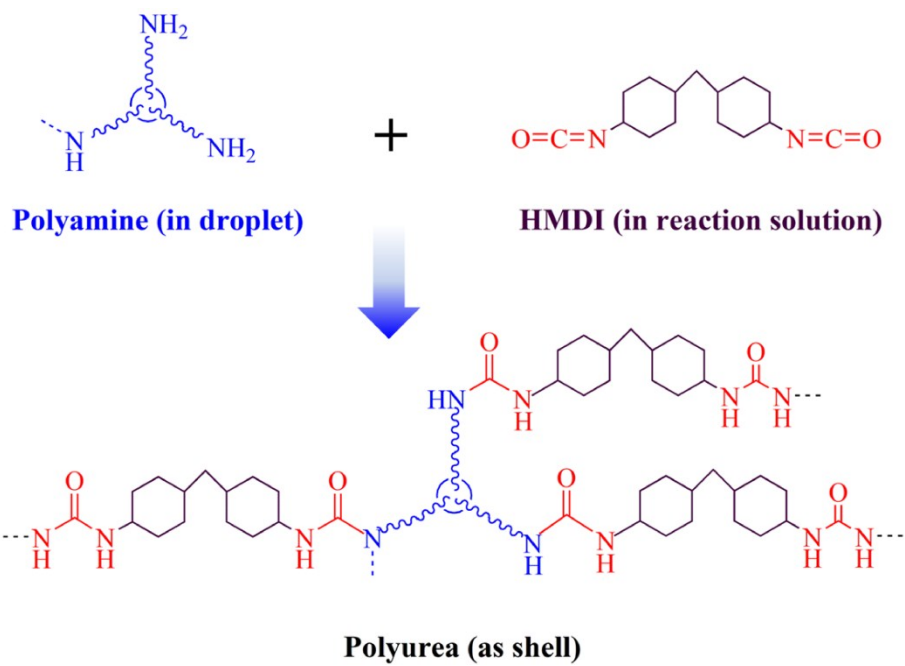
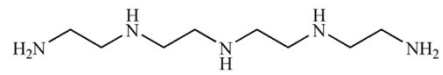
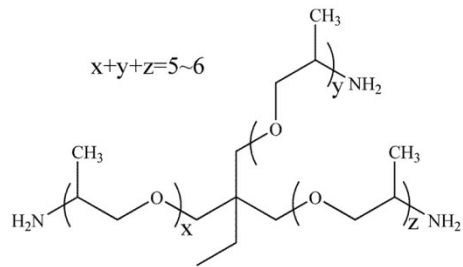


Fig. S1



TEPA



JEFFAMINE T-403

Fig. S2

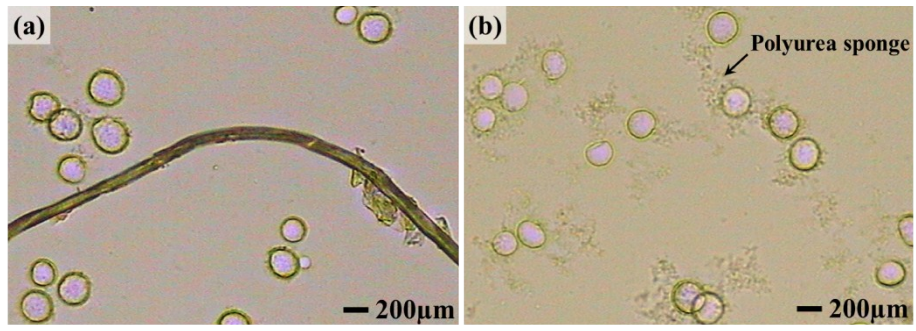


Fig. S3

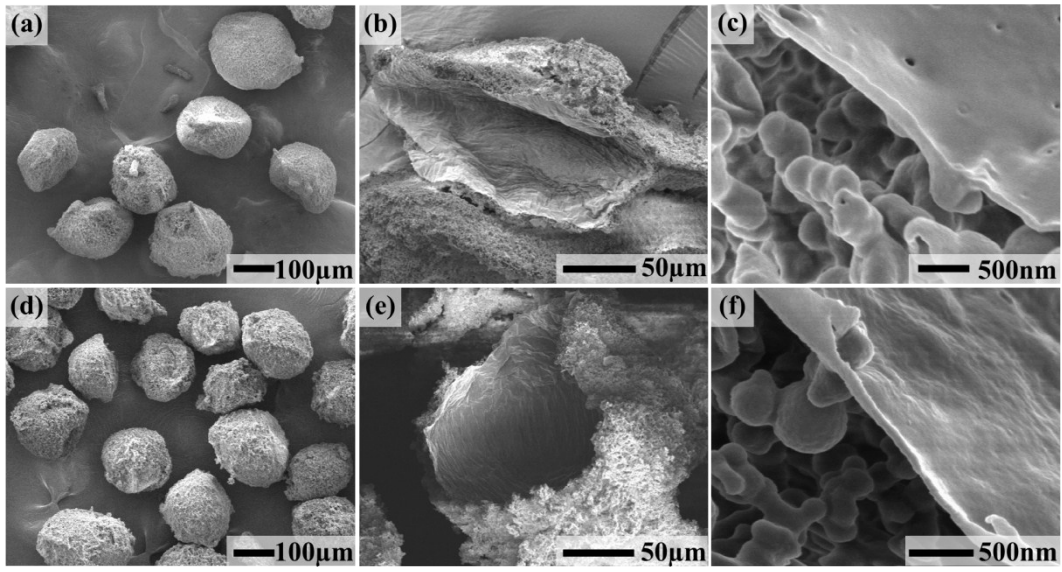


Fig. S4

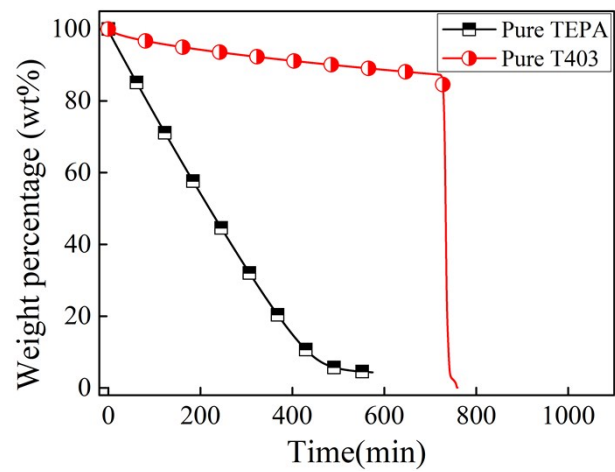
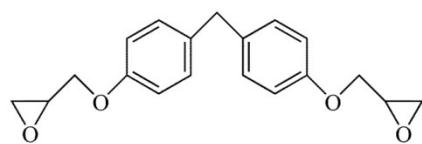
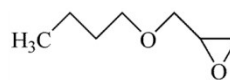


Fig. S5



BFDGE



BGE

Fig. S6

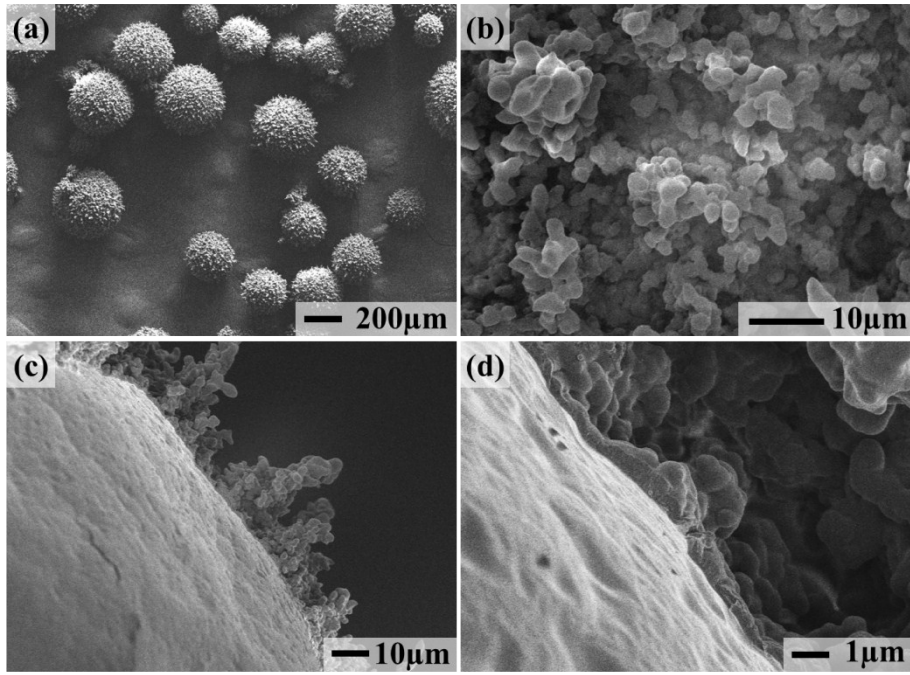


Fig. S7

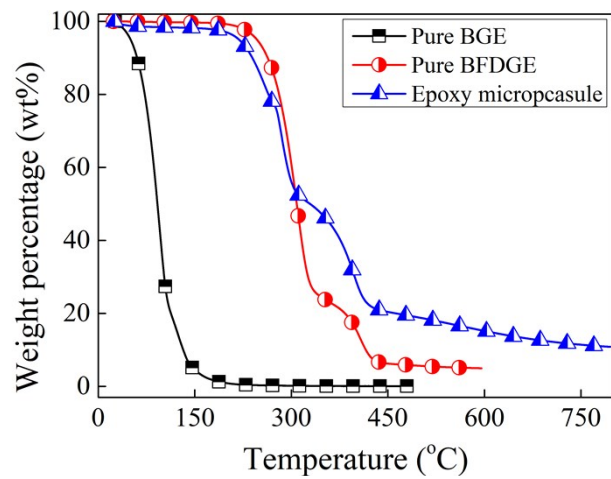


Fig. S8

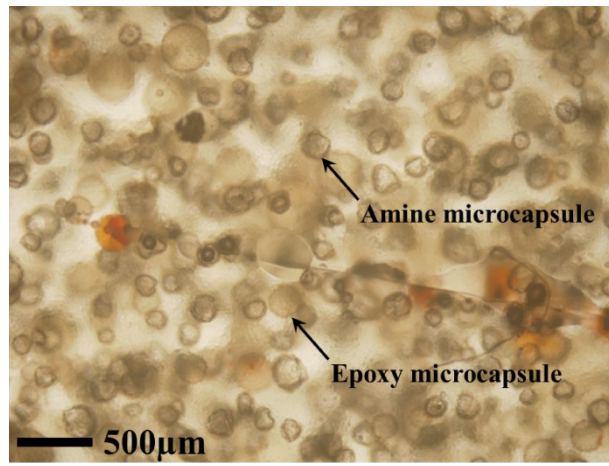


Fig. S9

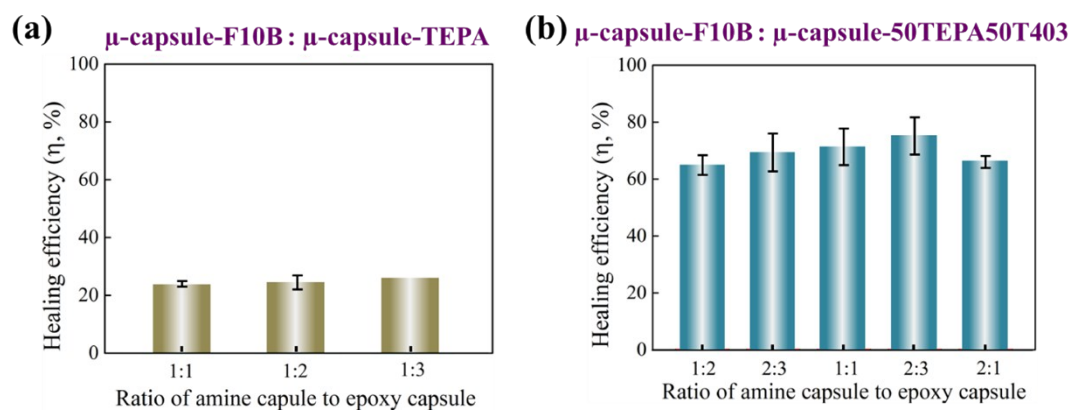


Fig. S10

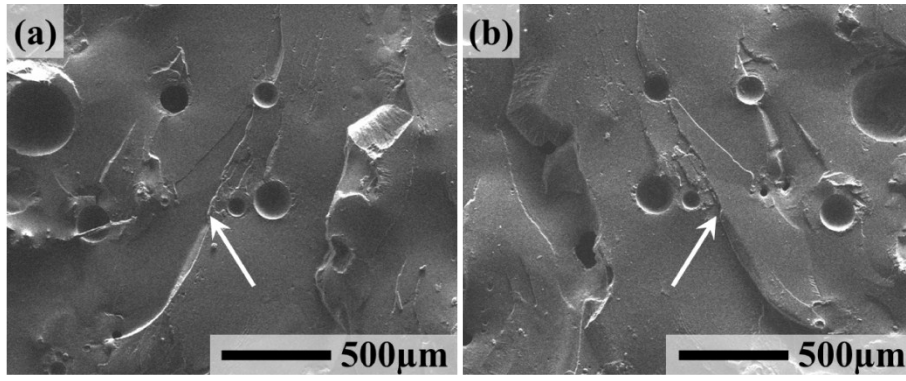


Fig. S11

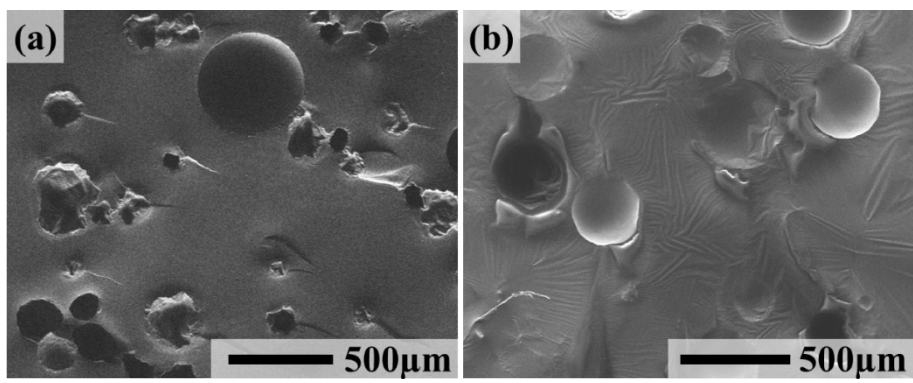


Fig. S12

Supplementary Table Caption

Table S1 Specific sample information using TDCB geometry for self-healing epoxy using encapsulated two-part amine-epoxy chemistry.

Table S1

Type of amine μ -capsule	Ratio of dual μ -capsule ^a	Total concentration (wt%)	Post-curing condition ^b	Healing duration at RT (h)	Ageing duration (month)
TEPA μ -capsule	2:1	10.0	T35-24h	48	0
	1:1	10.0	T35-24h	48	0
	1:2	10.0	T35-24h	48	0
	1:3	10.0	T35-24h	48	0
50TEPA50T403 μ -capsule	2:1	10.0	T35-24h	48	0
	3:2	10.0	T35-24h	48	0
	1:1	10.0	T35-24h	48	0
	2:3	10.0	T35-24h	48	0
	1:2	10.0	T35-24h	48	0
	2:1	10.0	T35-24h	48	0
	3:2	10.0	T35-24h	48	0
	1:1	10.0	T35-24h	48	0
	2:3	10.0	T35-24h	48	0
	1:2	10.0	T35-24h	48	0
25TEPA75T403 μ -capsule	1:1	0.0	T35-24h	48	0
	1:1	5.0	T35-24h	48	0
	1:1	7.5	T35-24h	48	0
	1:1	10.0	T35-24h	48	0
	1:1	12.5	T35-24h	48	0
	1:1	15.0	T35-24h	48	0
	1:1	10.0	T35-24h	48	0
	1:1	10.0	T60-24h	48	0
	1:1	10.0	T80-24h	48	0
	1:1	10.0	T35-24h	12	0
	1:1	10.0	T35-24h	24	0
	1:1	10.0	T35-24h	36	0
	1:1	10.0	T35-24h	48	0
	1:1	10.0	T35-24h	60	0
	1:1	10.0	T35-24h	72	0
	1:1	10.0	T35-24h	80	0
	1:1	10.0	T35-24h	48	0
	1:1	10.0	T35-24h	48	2
	1:1	10.0	T35-24h	48	4
	1:1	10.0	T35-24h	48	6
1:1	10.0	T35-24h	48	8	
1:1	10.0	T35-24h	48	10	
1:1	10.0	T35-24h	48	12	

^a Ratio of amine microcapsule to epoxy microcapsule. Epoxy microcapsule contains F10B;

^b All the specimens were firstly cured at RT for 24h; T35 means 35°C, and similarly hereinafter.

Supplementary Video Captions

Video S1 Thin continuous polyamine stream right after the microfluidic T-junction.

Video S2 Breaking down of thin continuous polyamine stream into individual droplets in T2 after the microfluidic T-junction.

Video S3 Individual polyamine droplets at end of T2 before getting into reaction solution.

Video S4 Evolution of polyamine droplet to microcapsule with preliminary polyurea membrane upon flowing of the mixture from T2 into reaction solution.

Supplementary References

1. H. H. Jin, C. L. Mangun, D. S. Stradley, J. S. Moore, N. R. Sottos and S. R. White, *Polymer*, 2012, **53**, 581-587.
2. D. Sun, Y. B. Chong, K. Chen and J. Yang, *Chem. Eng. J.*, 2018, **346**, 289-297.
3. J. D. Rule, N. R. Sottos and S. R. White, *Polymer*, 2007, **48**, 3520-3529.
4. E. N. Brown, M. R. Kessler, N. R. Sottos and S. R. White, *J. Microencapsul.*, 2003, **20**, 719-730.